

DESY SR-79/01  
January 1979

DESY-Bibliothek  
- 9. FEB. 1979

DETERMINATION OF CRYSTALLITE DIMENSIONS USING  
SYNCHROTRON RADIATION X-RAY DIFFRACTION PHOTOGRAPHS

by

Z. H. Kalman and I. T. Steinberger

*Racah Institute of Physics  
The Hebrew University of Jerusalem, Israel*

S. S. Hasnain

*Deutsches Elektronen-Synchrotron DESY, Hamburg*

To be sure that your preprints are promptly included in the  
HIGH ENERGY PHYSICS INDEX ,  
send them to the following address ( if possible by air mail ) :

DESY  
Bibliothek  
Notkestrasse 85  
2 Hamburg 52  
Germany

DETERMINATION OF CRYSTALLITE DIMENSIONS USING  
SYNCHROTRON RADIATION X-RAY DIFFRACTION PHOTOGRAPHS

Z. H. Kalman and I. T. Steinberger  
Racah Institute of Physics  
The Hebrew University of Jerusalem, Israel

S. S. Hasnain<sup>†</sup>  
Deutsches Elektronen-Synchrotron DESY, Hamburg

Abstract

*Synchrotron radiation Laue patterns give valuable information on the sizes and shapes of grains in a polycrystalline material even if these are too small for synchrotron topography. A calculation, based on kinematic theory, is presented for the radial and lateral broadening of the diffraction spots obtained with white radiation. The most conspicuous broadening is to be expected when the dimensions of the reflecting planes are small and not their number; this is at variance with the conditions leading to broadening observed with conventional monochromatic methods. Quantitative assessment of the crystal dimensions is possible if auxiliary spectral information is obtained by using selectively absorbing filters. The theory was applied to the analysis of Laue photographs of xenon and krypton crystallites condensed on a cooled beryllium substrate. Crystal dimensions down to a few nanometers could be determined. The method is, in principle, applicable to the determination of the grain size and shape distribution of fine grained polycrystalline samples of any material. Changes during crystallisation and recrystallisation can be easily followed by virtue of the simple experimental set-up and short exposure times involved.*

1. Introduction.

The standard methods for determining grain size and grain size distribution are based on powder line broadening and line profile analysis respectively (Warren and Averbach 1950). The measured intensities are always due to reflections from a large number of crystallites in different orientations; furthermore the diffraction broadening depends in these cases only on the linear dimension of the crystallites in the direction perpendicular to the reflecting plane, which may result in ambiguous interpretation if certain crystal habits are present. In addition the problem of experimental determination of the line profile tails presents well known difficulties.

It will be shown that some of these difficulties can be solved by employing synchrotron radiation for powder photography: With this method the sample is kept stationary and the number of irradiated crystallites may - or rather should - be quite small. Most of the crystallites will reflect (many will give more than one reflection spot) due to the continuous spectrum of the primary radiation. The high intensity ensures small exposure times. The resulting photograph is essentially a collection of single crystal photographs, and if the cross section of the primary beam is sufficiently small, the spots are well resolved. The diffraction broadening of each spot is due to the shape of one single crystallite. If the sample contains larger crystallites, the shape of the spot and its fine structure is indicative of crystal shape and of structure imperfections. The central conclusion of this paper is the observation that with well-collimated white primary radiation geometric diffraction broadening is determined by the dimensions of the reflecting planes and not by their number, i.e.

<sup>†</sup>Present address: Depart. of Chemistry, The University, Manchester, U.K.

by the two crystallite dimensions not affecting diffraction broadening of monochromatic radiation. If the respective wavelength range is known, the thickness of the platelets can be calculated from the broadening. However, the broadening prevents the observation of synchrotron radiation Laue topographs of thin crystal platelets at certain orientations.

The essentials of this argument can be readily understood by means of the Ewald constructions of Fig. 1. In the upper part of the figure the 410 reciprocal point is elongated due to the fact that the number of reflecting planes is small. In this case the extreme reflected rays ( $S_1'$  and  $S_2'$ , of wavelengths  $\lambda_1'$  and  $\lambda_2'$  respectively) will be exactly parallel and no broadening is expected with a stationary crystal and exactly parallel incident beam. The only influence of the number of reflecting planes will be on the spectral spread of the reflected ray; the fewer planes, the wider the spectral range of the reflected radiation. The lower part of the figure represents the case when the reflecting planes 410 are narrow: here the angle between the extreme rays  $S_1$  and  $S_2$  (of wavelengths  $\lambda_1$  and  $\lambda_2$  respectively) will increase as the reflecting planes become narrower. Each intermediate reflected ray will correspond to another wavelength, thus the narrowness of the plane causes diffraction broadening with a spectral dispersion of the reflected rays in planes containing the incident beam.

On a photographic plate perpendicular to the incident beam radial streaks will appear.

Both the theory of this effect and its experimental observation will be presented below.

## 2. Theory.

The diffracted intensity of a (small) crystallite is essentially proportional to the lattice function  $|G|^2$

$$|G|^2 = \prod_{i=1}^3 \frac{\sin^2 N_i \underline{L} \cdot \underline{a}_i}{\sin^2 \underline{L} \cdot \underline{a}_i} \quad (1)$$

where the diffraction vector  $L$  is defined as

$$\underline{L} = (\underline{S}_1 - \underline{S}_0) k \cdot \pi \quad (2)$$

(Laue 1960).

$\underline{S}_0$  and  $\underline{S}_1$  are unit vectors in the direction of the primary and reflected beam respectively,  $\underline{a}_i$  ( $i=1,2,3$ ) are the elementary lattice translations of the crystallite.

$N_i$  is the number of elementary cells in the direction of  $\underline{a}_i$ .

$k$  is the reciprocal wavelength.

We assume a polychromatic and perfectly parallel primary beam in the direction  $\underline{S}_0$  impinging on a crystallographic plane (H00) of an arbitrarily chosen crystallite at a glancing angle  $\phi$ . It is assumed that the primary spectrum contains the wavelength  $\lambda_\phi = \frac{1}{k_\phi}$  which fulfills the Bragg condition for  $\phi$  and the  $d$  value corresponding to the plane H. For simplicity assume an orthorhombic crystallite and a reflection of the type H00. Also assume that the edges of the crystal are parallel to the edges of the unit cell, and <sup>are</sup> of lengths  $A_1$ ,  $A_2$  and  $A_3$  such that  $A_i = N_i a_i$

A Cartesian coordinate system  $\underline{i} \underline{j} \underline{k}$  is chosen in such a way that  $\underline{i} = \underline{S}_0$  and the normal to the reflecting plane lies in the  $\underline{i} \underline{j}$  plane. Furthermore we assume the crystallite to be oriented so that  $\underline{a}_3$  is parallel to  $\underline{k}$ . Thus we have

$$\underline{a}_1 = a_1 (-\sin\phi \cdot \underline{i} + \cos\phi \cdot \underline{j}) \tag{3}$$

$$\underline{a}_2 = a_2 (\cos\phi \cdot \underline{i} + \sin\phi \cdot \underline{j})$$

$$\underline{a}_3 = a_3 \cdot \underline{k}$$

$\underline{S}_1$  will be approximately in the direction of the specular reflexion:

$$\underline{S}_1 = \cos(2\phi + \eta) \cdot \underline{i} + \sin(2\phi + \eta) \cdot \underline{j} + \epsilon \cdot \underline{k} \tag{4}$$

$\eta$  and  $\epsilon$  being small angles.

The wavelengths involved in the reflexion are close to  $\lambda_\phi$ .

Consider a wavenumber  $k_\phi + \kappa$ , with  $\kappa \ll k_\phi$ . Neglecting higher powers of the small quantities we have from (2) and (4)

$$\underline{L} = \{ [-2(k_\phi + \kappa) \sin^2\phi - \eta k_\phi \sin 2\phi] \underline{i} + [(k_\phi + \kappa) \sin 2\phi + \eta k_\phi \cos 2\phi] \underline{j} + \epsilon k_\phi \underline{k} \} \cdot \pi \tag{5}$$

$$\underline{L} \cdot \underline{a}_1 = \pi \cdot a_1 [2(k_\phi + \kappa) \sin\phi + \eta k_\phi \cos\phi] = \pi [H + 2a_1 \kappa \sin\phi + a_1 \eta k_\phi \cos\phi] \tag{6a}$$

$$\underline{L} \cdot \underline{a}_2 = -\pi a_2 \eta k_\phi \sin\phi \tag{6b}$$

$$\underline{L} \cdot \underline{a}_3 = \pi a_3 \epsilon k_\phi \tag{6c}$$

The width of a diffraction spot is conventionally defined by the interval between the first zeros about the corresponding principal maximum of Eq. 1:

$$-\frac{\pi}{N_i} < \Delta (\underline{L} \cdot \underline{a}_i) < \frac{\pi}{N_i} \quad (i=1,2,3) \tag{7}$$

Eq. 7 is actually a set of three conditions that must be simultaneously fulfilled by the variables  $\epsilon, \eta$  and  $\kappa$  of Eqs. 6a,b and c. The particular conditions for the wavelength range  $\lambda_\phi + \Delta\lambda$  and the angular ranges  $\pm\Delta\epsilon$  and  $\phi \pm \Delta\eta$  are obtained by substituting from Eqs. (6a,b and c) into

$$\text{Eq. (7): } \frac{\Delta\lambda}{\lambda_\phi} = \frac{\Delta\kappa}{k_\phi} = \frac{\Delta\eta}{2} \cot\phi + \frac{\lambda_\phi}{2A_1 \sin\phi} = \frac{\Delta\eta}{2} \cot\phi + \frac{1}{HN_1} \tag{8a}$$

$$\Delta\eta = \frac{\lambda_\phi}{A_2 \sin\phi} \tag{8b}$$

$$\Delta\epsilon = \frac{\lambda_\phi}{A_3} \tag{8c}$$

The above ranges will be the observed ones provided there are no other restrictions on the wavelength range. If the spectrum of the incident radiation is sufficiently broad,  $\Delta\eta$  is determined from (8b) and the wavelength range of the reflected rays can be calculated in turn from (8a). If, however, the spectrum of the incident radiation is narrower one has to substitute for  $\Delta\kappa$  in (8a) the actual spectral range of the source,  $\Delta\eta$  is determined by (8a) and it becomes less than predicted by (8b).

Some specific cases will now be considered:

- a) All dimensions of the crystallite are large, i.e.,  $N_i \gg 1$  for  $i=1,2,3$ . With very large  $N_i$  -s one obtains  $\Delta\epsilon = \Delta\eta = \frac{\Delta\kappa}{k} = 0$ ; the reflected beam has no angular divergence and it is monochromatic.
- b)  $N_3$  is small but  $N_1$  and  $N_2$  are large enough so that (8b) and (8a) yield  $\Delta\eta = 0$  and  $\frac{\Delta\kappa}{k} = 0$ . There will be an angular divergence due to  $\Delta\epsilon = \frac{2\lambda_\phi}{A_3}$  (8c). On a photographic plate perpendicularly to the incident beam there will be broadening in the direction perpendicular to the line containing the central spot and the diffraction spot in question ("lateral broadening"). Each broadened spot is made by monochromatic radiation of wavelength  $\lambda_\phi$ , satisfying the Bragg condition.
- c)  $N_2$  is small but  $N_1$  and  $N_3$  are larger enough to yield

$$\frac{\Delta\kappa}{k} = \frac{\Delta\eta}{2} \cot\phi \tag{9}$$

$$\Delta\epsilon = 0 \tag{10}$$

The third condition is given by (8b),  $\Delta\eta = \frac{\lambda_\phi}{A_2 \sin\phi}$ . In this case (6a) yields a one-to one correspondence between the wave

number  $k_\phi + \kappa$  and the reflexion angle  $2\phi + \eta$  :

$$\frac{\kappa}{k_\phi} + \frac{\eta}{2} \cot \phi = 0 \quad \dots\dots\dots(11)$$

This can be also written as

$$H \cdot (\lambda_\phi + \delta\lambda) = 2a_1 \sin \frac{2\phi + \eta}{2}$$

This is the Bragg equation for the reflexion angle  $2\phi + \eta$  with the wavelength  $\lambda_\phi + \delta\lambda$ . It should be noted that notwithstanding this the angle of incidence is  $\phi$ .

Equation 11 can be solved for any  $\eta$  within the interval  $\Delta\eta$  as given by (8b) provided the corresponding  $\kappa$  (as calculated from (10)) is within the spectral range  $\Delta\kappa_0$  of the primary radiation. Otherwise  $\Delta\kappa_0$  will delimit the possible values of  $\kappa$  and thus of  $\eta$  as well.

The reflected beam diverges by the angle  $\Delta\eta$  within the plane containing  $\underline{S}_0$  and  $\underline{S}_1$ ; on a photographic plate perpendicular to the incident beam there will be broadening along the line connecting the spot in question with the central spot ("longitudinal" or "radial" broadening). Every ray within this broadened pencil is of a single wavelength  $\lambda_\phi + \delta\lambda$ . This is the case depicted in the lower part of Fig. 1.

d) If  $N_1$  is small but  $N_2$  and  $N_3$  are large enough then

$$\Delta\epsilon = \Delta\eta = 0 \quad \text{and} \quad \frac{\Delta\kappa}{k_\phi} \quad \text{satisfies}$$

$$\frac{\Delta\lambda}{\lambda_\phi} = \frac{\Delta\kappa}{k_\phi} = \frac{1}{HN_1}$$

There will be no broadening in this case, but the reflected beam is polychromatic as given by the above equation. This is the case of the upper part of Fig. 1. Note, however, that now the number of reflecting planes is small. With such a habit and orientation one would observe the conventional angular broadening on powder or oscillation photographs using monochromatic radiation.

Of the cases listed above, "c" is the most interesting one.

In principle, Eq. (8b) yields the crystal thickness  $A_2$ .  $\phi$  and  $\Delta\eta$  are readily measured from the geometry; to find  $\lambda_\phi$  further information is necessary. This can be obtained by using a suitable absorption filter. The absorption edge of such a filter causes a cut off to appear on radial streaks at a radial distance corresponding by the scattering angle  $2\phi + \eta$ ;  $\eta$ , in turn, is given by the Bragg equation 11'. Thus a dark ring will cut off the radial streaks. This "eclipsed Debye-Scherrer circle" may also be observed as a result of the absorption edge of an element of the material investigated. In these cases the eclipse fades out towards the center as the absorption coefficient decreases (Fig.4). Bromine and silver contained in the photographic emulsion may also generate such circles, but in these cases the eclipse fades out away from the center (Fig.5).

The "negative circle" will be sharply defined and the streaks cut off abruptly if conditions "c" ( $N_2$  small but  $N_1$  and  $N_3$  large) prevail. The edge of the circle will be less sharp if  $\frac{1}{HN_1}$  cannot be neglected in (8a), i.e., if the number of the reflecting planes also becomes small. On the other hand, if  $N_2$  and  $N_3$  are small but  $N_1$  large the radial streaks will be broadened laterally because of the non-negligible value of  $\Delta\epsilon$  obtained from (8c).

It should also be noted that if the radiation source includes wavelengths appropriate for higher-order reflexions as well, streaky reflections not interrupted by the absorption edge will be superimposed on the main pattern.

3. Experimental. Solid xenon and krypton samples were condensed upon a cooled beryllium window. The window was part of an inner closed cell located in a vacuum cryostat. This arrangement enabled the investigation of samples at temperatures up to the vicinity of their melting point notwithstanding the very high vapour pressures. White radiation from the DESY electron synchrotron, run typically at 7.1 GeV and at a current of 6 to 8 mA, emerged from the beamline through a beryllium window into a 1.5 m air path, passed through the entrance window of the cryostat and that of the inner cell (both mylar, 50 μm thick). The diffracted radiation had to pass the cooled Be rear window of the cell and the mylar rear window (50 μm thick) of the cryostat before reaching either a Polaroid film or a nuclear plate (25 μm or 50 μm emulsion) held perpendicularly to the incident beam at a distance of 10 to 20 cm from the sample. The geometry was such that reflexions at angles  $2\theta < 40^\circ$  could be recorded. The diameter of the cross section of the incident beam utilized was about 0.5 mm. Exposure time varied between a few tens of seconds to a few minutes.

Figs 2 and 3 refer to the same xenon sample, deposited at about 90°K and heated up gradually. Their behaviour is typical for all the samples (about 6) investigated; a detailed description of the crystal growth and recrystallisation will be published separately. At the lowest temperatures only very blurred Debye-Scherrer halos are seen. Fig. 2 was obtained when single crystal reflexions just started to appear, at about 140°K. The diffraction pattern consists of very many small spots and several large and broad radial streaks ("comets").

The very large number of small spots indicate that the incident beam encompassed many crystallites. It should be noted that most of the small spots are also elongated radially; careful inspection of the original photographs reveals that lateral broadening is also present\*. The spots are, on the whole, more elongated near the centre than at large scattering angles. This is in full accord with the predictions of Eq. 8b - the  $\sin\phi$  factor in the denominator enhances the elongation at small angles. Equations 8b, along with 8c, also served to estimate the size of the crystallites; it was found that typically  $A_2 \approx A_3 \approx 0.1 \mu\text{m}$ . The  $\sin\phi$  factor causes the radial broadening to be more pronounced than the lateral one.

The comet-like large streaks are, in fact, considerably more numerous than it seems from the printed reproduction of the figure. In the most prominent ones darker lines are observed, corresponding to eclipsed Bragg reflexions with wavelengths of the xenon or silver K-edge and d-values of xenon (1 1 1), (2 0 0), (2 2 0) and (3 1 1) planes. These suppressed reflexions introduce a wavelength scale on the photograph, with  $\lambda$  increasing from the centre outwards. In fact, this scale was used in interpreting the small spots (see above) as well. It was found that both the width and length of the streaks is indicative of crystallites having the dimensions  $A_2 \approx A_3 \approx 3 \text{ nm}$ . The comet-like gradual widening of the streaks with the increase of the distance from the centre is in full accord with the prediction of Eq. 8c, taking into account the increase of the wavelength  $\lambda\phi$  with the increase of the distance from the centre. The high intensity of some of the "comets" may be due to well-aligned aggregates of the small crystals, though most photographs were more or less over-exposed and, therefore, the intensities could not be reliably compared.

---

\*Very similar spots were observed by McCormack and Tanner (1978, Fig. 1b) for fine grain silicon steel.

Summing up, it follows that the sample of Fig. 2 consisted of two kinds of crystallites, of widely different dimensions: one kind of the typical dimensions of a few nanometers while the dimensions of the others were of the order of a hundred nanometers. The distribution of the diffraction spots is roughly uniform on the photograph; one may infer that there is no pronounced preferred orientation.

Fig. 3 represents the same sample at a higher temperature after it underwent recrystallisation. It is clearly seen that the number of reflexion spots decreased considerably. The "comets" disappeared but the remaining spots are, on the whole, much more elongated than the small spots of Figure 2. From their length one infers, according to 8b, that  $A_2$  varies from 10 to 20nm; their width yields  $10\text{nm} < A_3 < 100\text{nm}$ . Since we deal with rather small reflexion angles ( $2\phi < 15^\circ$  in this case), the reflecting planes are roughly parallel to the incident radiation and perpendicular to the beryllium substrate; the above results about  $A_2$  and  $A_3$  indicate that many crystals are platelets  $\sim 10\text{nm}$  thick and  $\sim 100\text{nm}$  in their other dimensions, approximately parallel to the beryllium substrate. It should also be noted that the central spot is surrounded by a dark "shadow": though the outer limit of this eclipsed region is not quite sharply defined, it was found - as in dozens of other photographs - that this limit corresponds to the (1 1 1) fcc Bragg reflexion for the wavelength of the xenon absorption edge. Such a clear "shadow" can be present only if there is a high degree of preferred orientation about an axis approximately parallel to the primary beam; otherwise, reflexions with smaller d-values and wavelengths considerably below the absorption edge may appear anywhere within the eclipsed region washing out the edge.

Obviously, considerable recrystallisation took place between obtaining Fig. 2 and Fig. 3, involving rearrangement of directions.

The fact that only a few larger crystals were present is seen in Fig. 3 in two more ways: a) in many streaks some internal structure can be discerned manifested mainly by uneven intensity distribution. This is probably due to low-angle grain boundaries within the individual crystallites; b) a part of Laue zone ( $\approx 100^\circ$ ) is seen near the periphery of the photograph. All reflexions of this zone are due to the same crystal.

Careful study of Fig. 3 reveals that there are further eclipsed Bragg reflexions on the photograph, corresponding to other d-values. However, this effect is much clearer in Fig. 4. It was obtained on another xenon sample. Radial streaks are evident throughout as well as eclipsed reflexions, i.e., superimposed dark rings. From the geometry, it was found that in the angles of  $\phi_{\text{HKL}}$  the rings satisfy the Bragg condition  $2d_{\text{HKL}} \sin \phi_{\text{HKL}} = \lambda_{\text{xe}}$  where  $\lambda_{\text{xe}}$  is the K absorption edge ( $\lambda_{\text{xe}} = 0.3578\text{\AA}$ ) of xenon and HKL refer to the cubic reflexions (1 1 1), (2 0 0), (2 2 0), (3 1 1) and (3 3 1) respectively (the last ring is not well reproduced in the enlargement). Measuring the lengths and widths of the streaks reveals, using 8b and 8c, that  $A_2$  varies between 10 and 20nm while  $A_3$  is in most cases of the order of 100nm.

For the thickest streaks,  $A_3 \approx 20\text{nm}$ . The sharp cutoff of the rings is consistent (through Eq. 8a) with this estimate of the crystal breadths. In this case, the existence of preferred orientation is even more obvious than in Fig. 3; as all the reflecting planes belong to the [1 1 0] zone, it follows that this axis is roughly parallel to the incident beam and perpendicular to the substrate. Incidentally, the fact that this is the preferred orientation

precludes attributing the streaks to one-dimensional stacking disorder of (111) planes.

In Fig. 5, a similar diffraction pattern is presented for krypton crystallites. In this case, three dark rings are observed, corresponding to (111) reflexions of fcc krypton eclipsed by the Ag, Kr and Br K-absorption edges and a further ring due to the (200) krypton reflexion eclipsed due to the Kr K-edge. The Ag and Br eclipses fade out from the centre outwards, as expected, while the Kr eclipses behave as those due to Xe in Figs. 2, 3 and 4. Measuring the streak dimensions revealed that, in most cases, all dimensions of the crystallites are less than 10nm.

A counterexample for the above presented patterns appears in Fig. 6. This refers to a xenon sample two or three minutes before its total disappearance due to sublimation. Streaks appear in this case as well; but they are not straight as in the previous cases, but curved like the central portion of an oscillation photograph obtained by white radiation. In fact, subliming solid xenon samples very often are seen to vibrate in their container, when heated from the outside, due to periodic variation of the thermal contact with the walls.

#### 4. Conclusions.

X-ray topography by synchrotron radiation has been established as a simple and fast method for the assessment of various crystal defects (Tanner, 1977). It can also conveniently serve for the study of changes of the crystal size, structure, and habit during crystallisation and recrystallisation (McCormack and Tanner, 1978; Steinberger, Kalman and Bordas, 1977). In the present work, it has been demonstrated that when the crystal

dimensions are much too small for topography, these dimensions can be estimated from analysing the radial and lateral broadening of the diffraction spots. In this way crystal dimensions of a few nanometers were found in the present work. The method may conveniently serve for grain size distribution studies in polycrystalline samples of almost any element or compound. The samples do not have to be thinned down as for transmission electron microscopy. Because of the simple experimental setup and short exposure times needed, the method is also applicable to "in situ" studies of crystallisation and recrystallisation.

#### Acknowledgments.

The authors wish to thank Dr. E. E. Koch and Dr. G. Materlik of DESY for their constant interest in the experimental work. One of the authors (I.T.S.) is acknowledging the support of the Minerva Foundation.

References

- Laue, M.v., (1960) ROENTGENSTRAHL INTERFERENZEN  
3rd Ed., Akademische Verlagsgesellschaft, Frankfurt/Main
- Mac Cormack, I.B., and Tanner B.K., (1978)  
J. Appl. Cryst., 11, 40.
- Steinberger, I.T., Bordas J. and Kalman Z.H., (1977)  
Phil. Mag., 35, 1257.
- Tanner, B.K. (1976): X-RAY DIFFRACTION TOPOGRAPHY  
Pergamon Press, Oxford.
- Warren, B.E. and Averbach B.L., (1950)  
J. Appl. Phys. 21, 595.

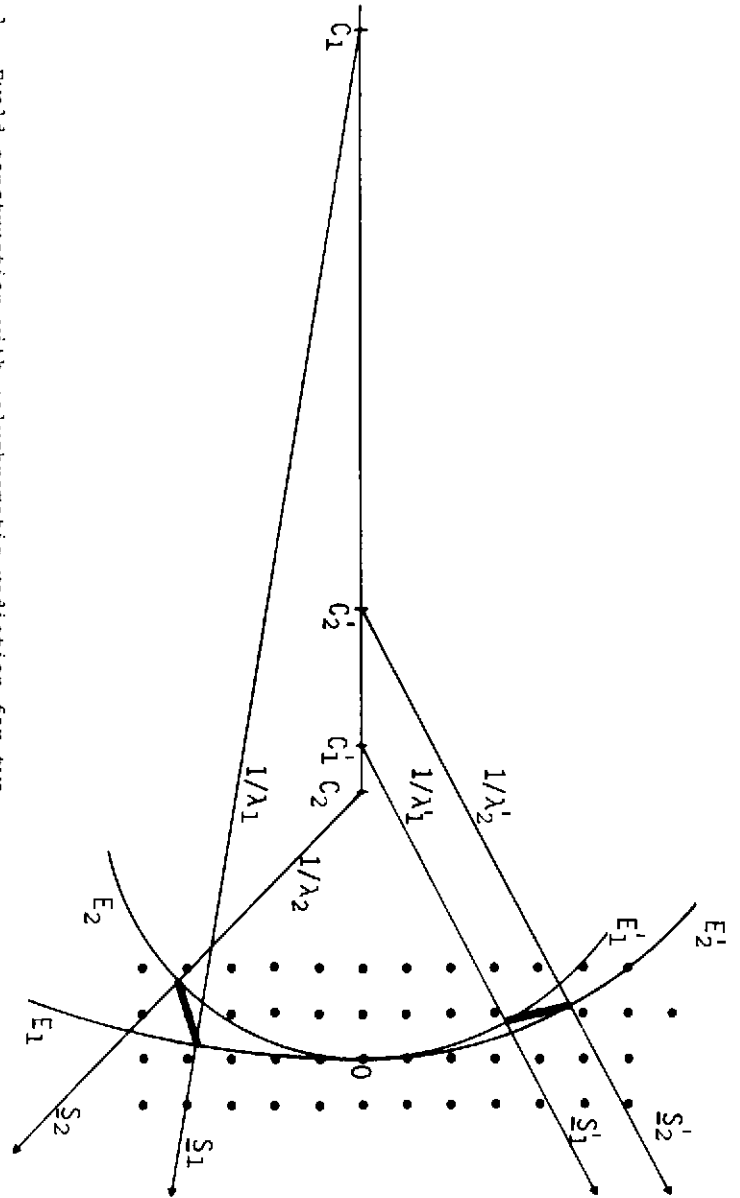


Fig. 1 Ewald construction with polychromatic radiation for two small crystallites. Upper half - the reciprocal lattice point is elongated in the direction of its reciprocal lattice vector; lower half - the elongation is perpendicular to the reciprocal lattice vector (narrow lattice planes).

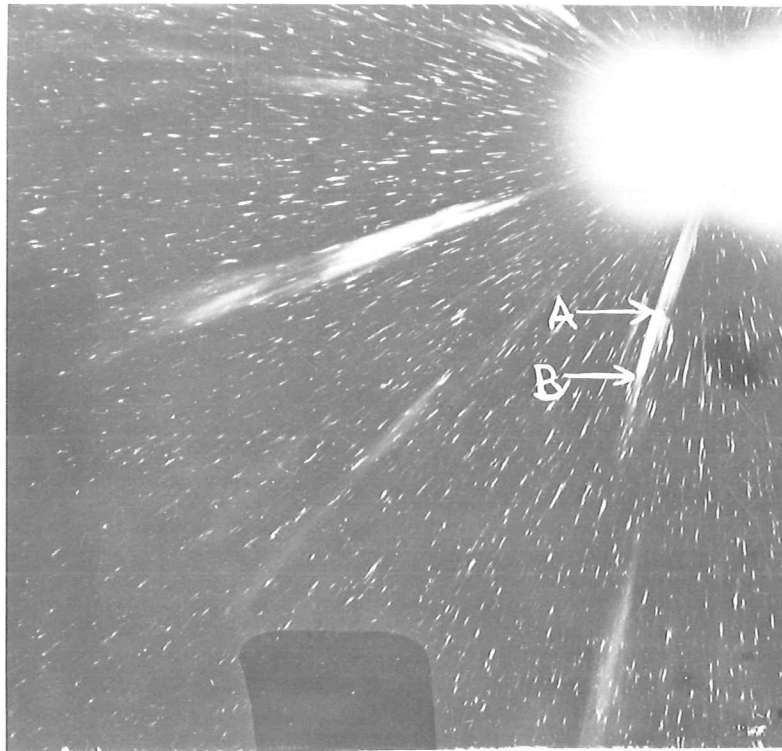


Fig. 2 Laue photograph of a polycrystalline xenon sample: Eclipsed (111) fcc reflexions are marked: A - for  $\lambda_{Xe} = 0.3578 \text{ \AA}$ ; B - for  $\lambda_{Ag} = 0.4858 \text{ \AA}$ .



Fig. 3 Laue photograph of the sample of Fig. 2 at a higher temperature, after recrystallization. Some reflexions belonging to the same Laue zone are marked by x.

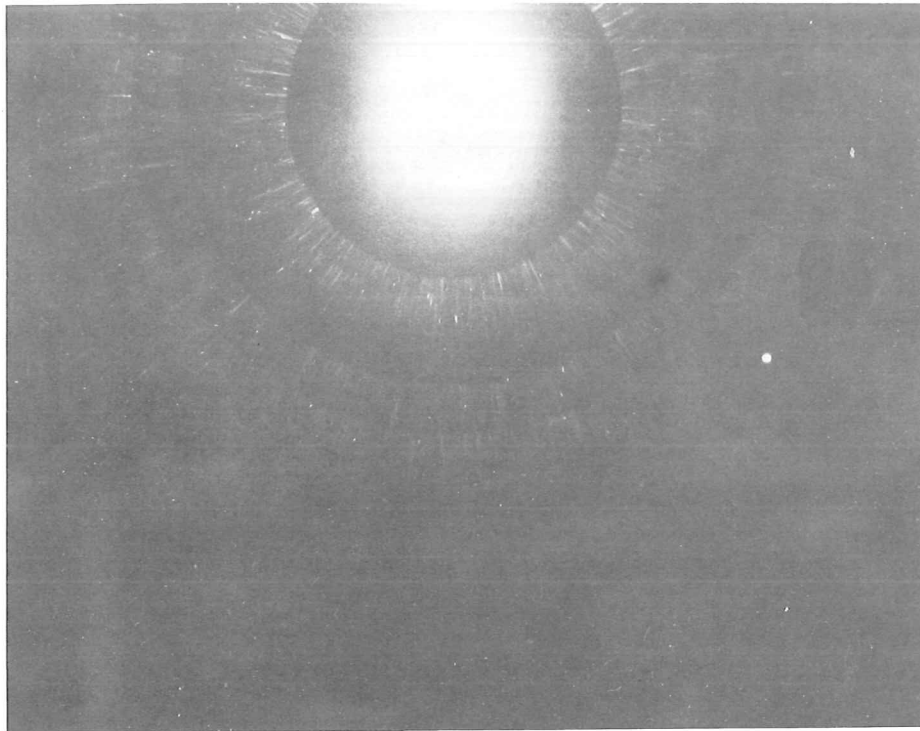


Fig. 4 As 2 or 3 for another xenon sample. The successive dark rings correspond (from the centre out) to the eclipsed fcc reflexions (111), (200), (220), (311) and (331) all for  $\lambda_{Xe} = 0.3578 \text{ \AA}$ .

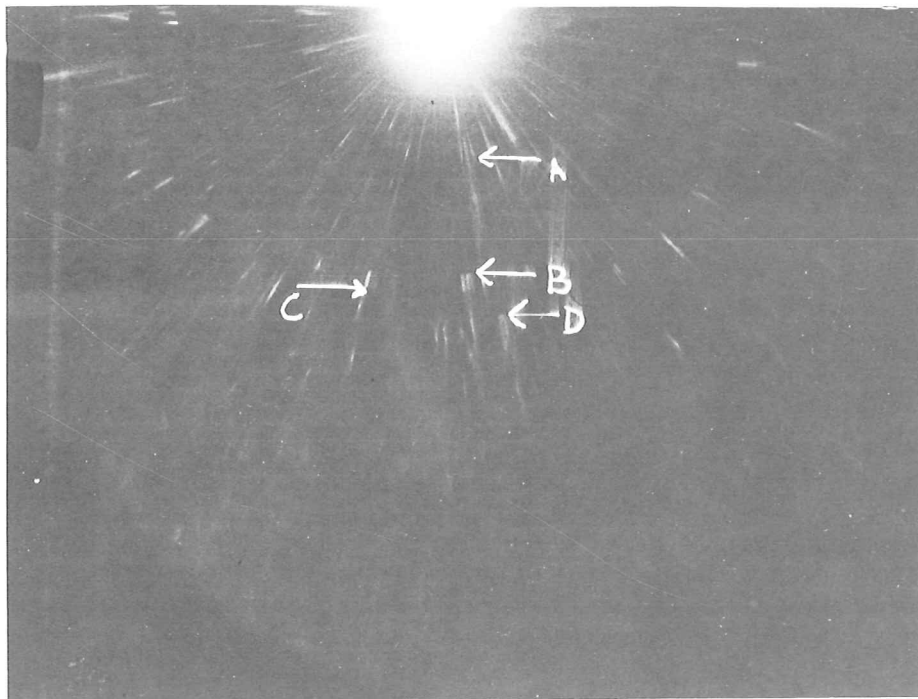


Fig. 5 Laue photograph of a polycrystalline krypton sample. Marked eclipsed fcc reflexions : A - (111) with  $\lambda_{Ag} = 0.4858 \text{ \AA}$   
 B - (111) with  $\lambda_{Kr} = 0.8655 \text{ \AA}$  , C - (111) <sup>Ag</sup> with  $\lambda_{Br} = 0.9200 \text{ \AA}$   
 and D - (200), again with  $\lambda_{Kr}$  .

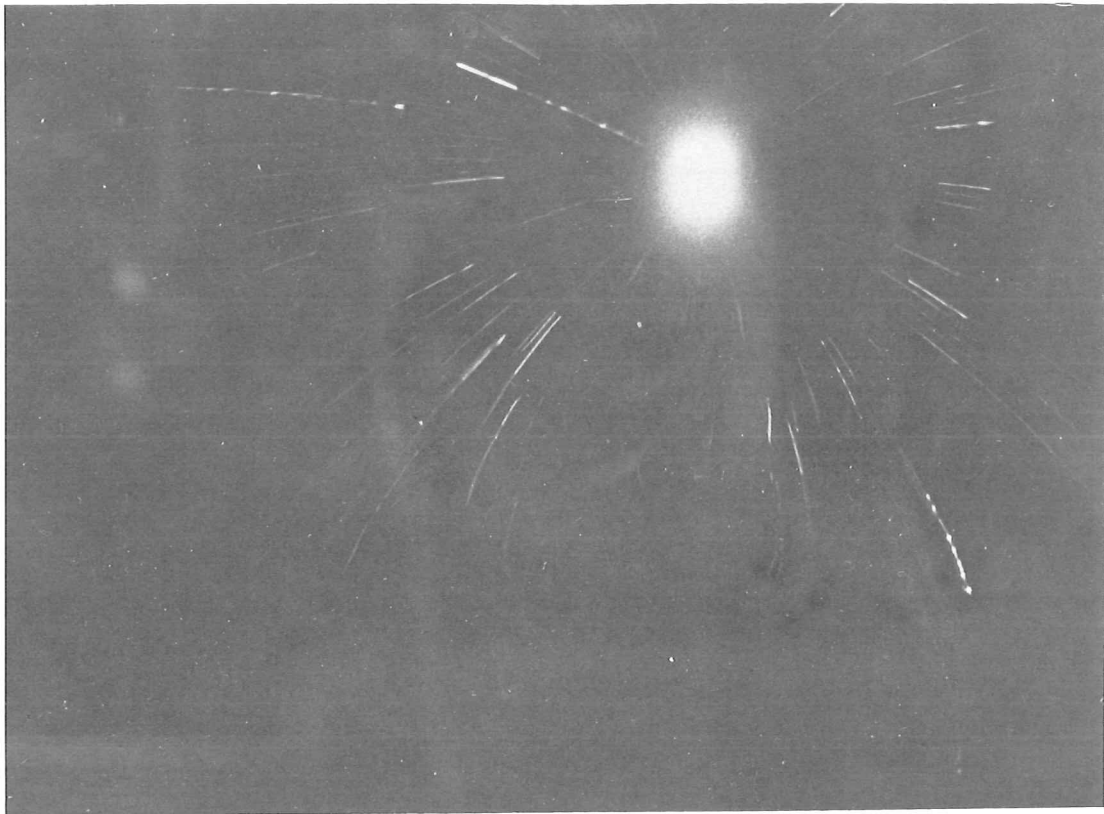


Fig. 6 White radiation X-ray photograph of a few crystallites just before their disappearance by sublimation, See text.